ELSEVIER

Journal of Power Sources 53 (1995) 351–357

JOURNAL OF POWER SOURCES

Computer model of the lead/acid starter battery in automobiles

H. Duval

University of Paris VI, Paris, France

Received 12 August 1994; accepted 3 September 1994

Abstract

A large increase in the power required on-board automobiles is expected in the years to come. More complex electric networks will then be required to provide adequate reliability and minimal fuel consumption. The scope of this study is to present a model for an automotive battery introduced in a software package that is developed to simulate current and future electrical architecture. This model is based on an evaluation of battery e.m.f., over-voltage and capacitive behaviour. A description is given of the test protocol used to develop laws and to validate the model. The model is tested successfully both in starting phases and under real vehicle running conditions.

Keywords: Lead/acid batteries; Model; Automobiles; Computer model; Starter batteries

1. Introduction

Nowadays, vehicle equipment is becoming more and more complex and a large number of units are supplied by the on-board electric network (e.g., heated windscreens, heated seats, power steering). This results in increasing complexity and variability of the electric networks (e.g., increase in the number of units to be power supplied, quality of the power supply, safety, harness complexity, etc.). One way to solve this problem is to use simulation tools. When simulation is applied to the electric network, the software [1] must provide time-based analysis of the key variables, such as currents and voltages of the alternator, battery and consumers, the battery state-of-charge (SOC), etc.

Each unit requires a specific study in order to model its behaviour, and is considered as a black box with various mechanical and/or electrical inputs and outputs that can be influenced by external parameters (battery temperature, for example). The input and output interrelations are turned into equations, with the assumption that the unit is used under normal operating conditions (e.g., typical temperature and voltage ranges recorded in a vehicle). Two standard approaches have been used:

(1) global modelling where the component behaviour is directly identified from test runs; this is a simple and fast method;

(ii) the physical approach, where the physical equations of the unit are defined; this is a more complex, but more rigorous and accurate, method.

Both approaches have been used given the importance of the component in the system to be simulated. The second has been applied to the battery. Given the priority targets for the simulation tool (namely, power balance and network behaviour analysis), only the quasi-stationary states of the components have been considered. Except in specific cases, transient models have not been taken into account and the simulation time step is deliberately limited to approximately 1 s.

2. Battery model

The battery black-box behavioural model (Fig. 1) has to run at temperatures between −20 and 60 °C to accommodate temperate climates. To describe this unit behaviour, states equations have been considered. These involve independent variables (U, I, SOC, Q) and are dedicated for the unit in question. The temperature is taken as a key determinant of battery behaviour. Thus:

$$F_T(U, I, Q, \mathrm{SOC}) = 0 \quad (1)$$

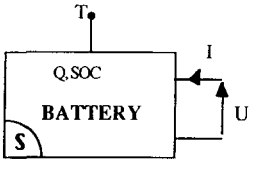

Fig. 1. Battery black box.

* Present address: Renault France, 9–11 Avenue du 18 Juin 1940, F-92500 Reuil Malmaison, France.

SSDI 0378-7753(94)02000-S

where U = battery voltage; I = charge current (negative during discharge); Q = delivered ampere hours; SOC = state of charge; T = electrolyte average temperature, measured just above the plate grids.

The physical equations are derived from studies of electrical and capacity behaviour. The determination and identificator of the coefficients are based on experimental results (see tests protocol, below).

2.1. Electrical behaviour

The electrical behaviour is referenced to the electromotive force 'e.m.f.' (in the sense of the electrochemical open-circuit voltage). The difference between this voltage with that at the battery terminals is assessed. The e.m.f. at 25 °C, E_{25}, is a fourth order polynomial (Covington's polynomial [2]) function of the molarity logarithm. The molarity, m, is assessed from the initial electrolyte filling conditions [3] and the ampere-hour output. Hence:

$$E_{25} = P^4[\log(m)] \tag{2}$$

where $m = F$ (initial state, Q). The dependence of the e.m.f. on temperature T under the operating conditions (no more than 50% of the nominal capacity can be discharge) of a 12 V starting battery is approximately 1.2 mV per °C [2]. Therefore:

$$E = E - 25 + 0.0012(T - 25) \tag{3}$$

The voltage discrepancy ΔU comprises an ohmic drop [2], a scatter component (Fick's law) and the charge transference (adaptation of the Butler–Volmer law) [4]. The law is then of the following type:

$$\Delta U = rI + V_1 \frac{|I|}{I} \log\left(1 + \frac{|I|}{D}\right) + V_2 \operatorname{arcsh}\left(\frac{BI}{S_{\text{avail}}}\right) \tag{4}$$

with $U = E + \Delta U$ and $I < 0$ under discharge, where r, V_1, V_2, B and D are temperature-related factors, and S_{avail} is the percentage of the surface available for the electron transfer.

The extreme sensitivity of these factors to measurement errors and/or discrepancies leads to a logarithmic interpolation between the voltage discrepancy values. The S_{avail} rate depends on the SOC under discharge; under charge it depends on the ampere-hour percentage output with respect to the maximum capacity C_0 (see below). The electrical behaviour depends, therefore, on the state of capacity.

2.2. Capacity behaviour

The state of capacity is affected by the output ampere-hour quantity, Q, the faradic efficiency (ratio between the real-current charging the battery and the efficient current), the steady state capacity $C(I,T)$, and the SOC. The quantity Q is the integral of the current weighted by the faradic efficiency η. The variation of constant temperature (25 °C) is a function of the ratio, r, between the output ampere-hour quantity and the nominal capacity (over 20 h). The efficiency h equals 1 when the ratio r is below 50% and is zero for 100%. Its characteristic curve reaches the value η_{80} at 80%. An exponential-type law is used to represent it, and changing η_{80} can be used to downgrade the output according to the temperature-related operating range [5] or the battery type (antimony, calcium, hybrid). The capacity $C(I,T)$ is a logarithmic type of law [6]. If the freezing phenomena are overlooked, the law reads as follows:

$$C = C_0 - C_1 \log\left(1 - \frac{I}{I_d}\right) \tag{5}$$

where C_0 = maximum battery capacity, irrespective of the temperature; C_1, I_d = temperature-related factors according to a second-order polynomial relation.

In addition, the SOC turns to discharge as a function of the ratio of the ampere-hour quantity immediately output ΔQd to the capacity $C(I,T)$ of the corresponding battery working conditions. Under charge, the ratio affects the ampere-hour quantity missing in the battery, Q, the quantity recharged ΔQd and the SOC. Times are generally expressed as tn-1 and tn, hence:

$$\text{SOC}_n = \text{SOC}_{n-1} - 100 \times \frac{\Delta Q\text{d}}{C(I,T)} \quad \text{under discharge} \tag{6}$$

$$\text{SOC}_n = \text{SOC}_{n-1} + \frac{\Delta Q\text{c}}{Q} \times (100 - \text{SOC}_{n-1}) \quad \text{under charge} \tag{7}$$

The model of the battery capacity and electrical behaviour has now been established, and the influence of the first on the second has been taken into account. It is now necessary to establish the empty battery criteria.

2.3. Empty battery criteria

The empty battery criteria depend on two factors: (i) temperature; (ii) discharge current level. The first one yields the minimum electrolyte density that can be reached if it is assumed that the battery is able to work under negative temperature. The temperature is measured and as the average molality is known (to evaluate the e.m.f.), a comparison can be made of the electrolyte composition and the corresponding freezing point [7]. The simulation is stopped when the freezing point is reached.

Under an average electrolyte running temperature, the discharge current level associated with the SOC evaluation gives a good indication of the battery capability to work under high current. It can be determined whether the thermal engine will start after different

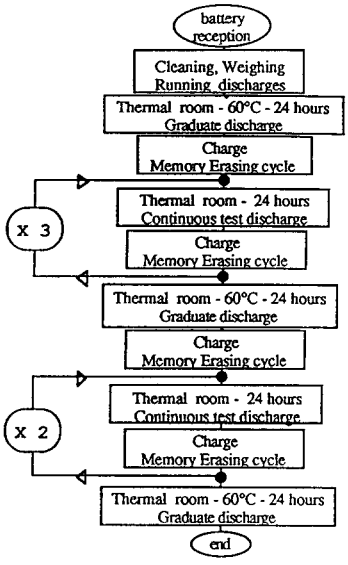

Fig. 2. Battery test procedure.

mission profiles that have been applied to the different circuit components. The global model has been validated under discharge for 50 Ah batteries (over 20 h) and a cold-start current of 250 A.

3. Experimental

An experimental protocol (see Fig. 2) has been developed to validate the model and to identify the different model parameters. To ensure a good reliability of the model and to avoid dispersions, ten batteries were selected. These were manufactured in the same batch and were filled to the same level with controlled density electrolyte. Before each utilization, each battery was cleaned, electrically equipped, and weighed (in order to determine water consumption by weight loss).

Before validation tests, running discharges ($I = C/20$, 20 °C) were conducted to ensure that batteries are tested fully charged and exactly in the same state. The discharge was followed by 14.8 V charges, except the last one which was under 16 V (gassing homogeneity). A comparison was made with the registered data and no significant deviations were observed. Two batteries were used simultaneously under different conditions. One battery was always in standby (it had already been submitted to running discharges).

Throughout the electrical operations, the electrolyte temperature, currents and voltages were registered. At the end of each charge and discharge, the battery was weighed (in order to measure the water consumption) and the electrolyte density was measured in each cell. To assess a good homogeneity, this last measure was compared with the e.m.f. voltage, after a rest period of 24 h. Some discharges were performed to control behaviour changes and/or to erase memory effects.

Following each test discharge, the batteries were charged for 12 h under 16 V (30 A max.) after a rest time of 24 h. Memory effects were avoided by discharging for 20 h at 25 °C and recharging under the same conditions. The water compensation was made during these cycles, called 'memory-erasing cycles'. The current, voltage and temperature were monitored in order to compare behaviour throughout the use of a given battery (Fig. 3). After the cycle, each battery was rested at room temperature for at least 24 h. The batteries were then transferred to a thermal room for 24 h in order to run future test discharges.

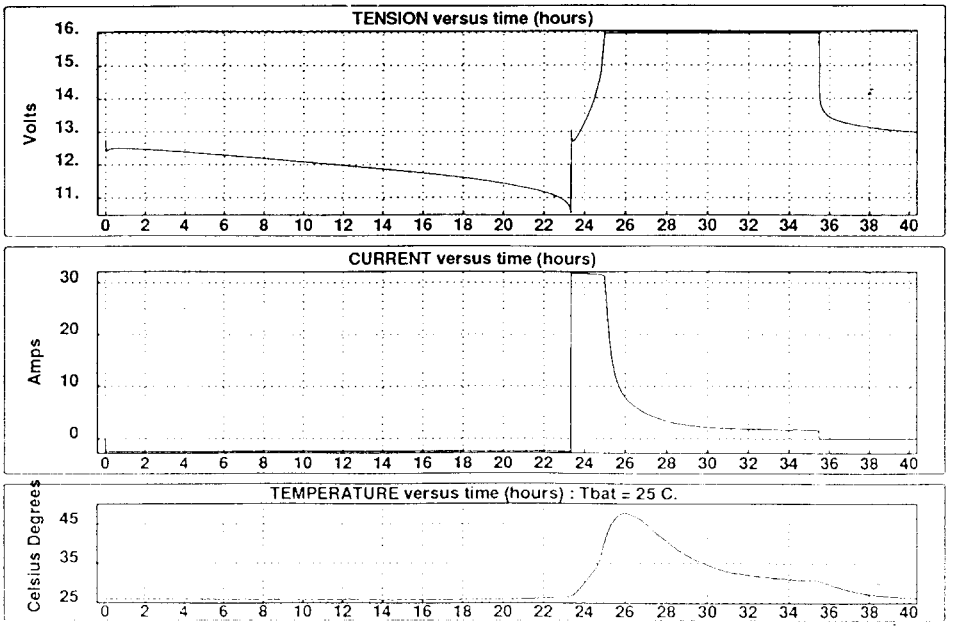

Fig. 3. Current, voltage and temperature of a battery during memory-erasing cycles.

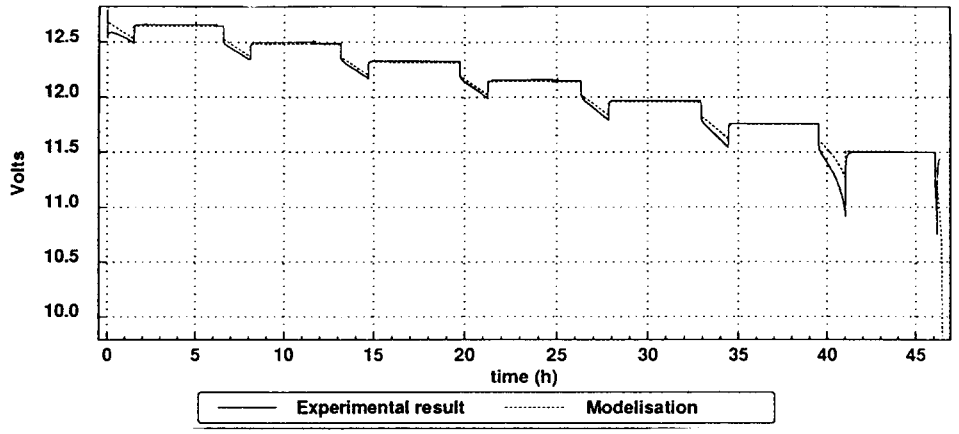

Fig. 4. Graduated discharge of a battery (temperature = 60 °C; discharge current 5 A).

Table 1
Validation of e.m.f. law [a]

Q (Ah)	Measured e.m.f. (V)	Calculated e.m.f. with compensation (V)
0	12.77	12.8
7.64	12.65	12.66
15.28	12.49	12.49
22.92	12.33	12.32
30.56	12.15	12.15
38.20	11.97	11.96
45.84	11.76	11.76
53.49	11.50	11.51

[a] To calculate the real e.m.f., water consumption and self-discharge are taken into account.

Table 2
Capacity law validation

T (°C)	Delivered currents (A)				
	2.5	5	20	50	80
Measured capacities (Ah)					
−20	36.2 [a]	31.1	21.1	16.8	
−10			26.8		
0	50.4	48.1	36.0	26.7	21.0
20	56.7	53.6	44.9	33.0	
40		55.6	46.7	39.3	
60	57.9		50.1	42.8	
Calculated capacities (Ah)					
−20	42	31	22	17	
−10			28		
0	53	48	36	27	22
20	57	54	44	34	
40		55	48	39	
60	58		51	43	

[a] Freezing electrolyte.

Each battery was subjected to three graduated discharges at 60 °C and 5 A in order to examine the e.m.f. law (Fig. 4). The first was performed immediately after the running discharges, the second after three full discharges and the third after two more full discharges. The capacity and voltages were compared to ensure that a reasonably new battery was being used. The capacity was in the range 56 Ah ± 3%.

If a battery presents suspect behaviour, it was substituted by the standby one. The suspect battery was subjected to a visual analysis of the internal parts (mechanical resistivity of the active materials, grid growth, corrosion of the internal connectors, faults, etc.) Immediately, another battery was taken from stock to conduct the running discharges.

Continuous test discharges were performed under several conditions at temperatures between −20 and 60 °C and currents from 80 to 2.5 A. The voltage limit was varied as a function of current and temperature [6].

A field of temperature was assigned to each battery. Thus, one battery experienced discharges at 0 °C, another at 20 °C, some at 40 °C, and one at high temperatures (60 °C and some at 40 °C). The first continuous test is conducted at a high level of discharge.

Three currents for each reference temperature (−20, 0 and 60 °C) were used to identify the model parameters. The choice depends on voltage drop (accuracy) and internal heating due to discharge conditions. The other tests were used to validate the behavioural laws.

4. Results and discussion

4.1. Validation of battery model

Fig. 5 gives a comparison between different discharges on the memory-erasing cycles. There are some deviations coming from differences in temperature and initial electrolyte density. In addition, degradation of the active material was observed due to high temperature (for one battery) or freezing electrolyte (low current, low temperature).

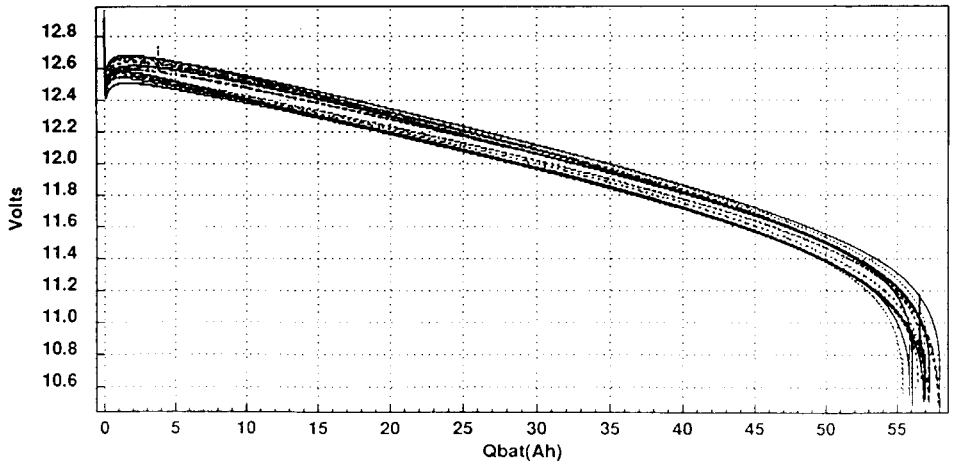

Fig. 5. Discharge during memory-erasing cycles. Battery voltage vs. output ampere-hours: $I=2.5$ A; $T=25$ °C.

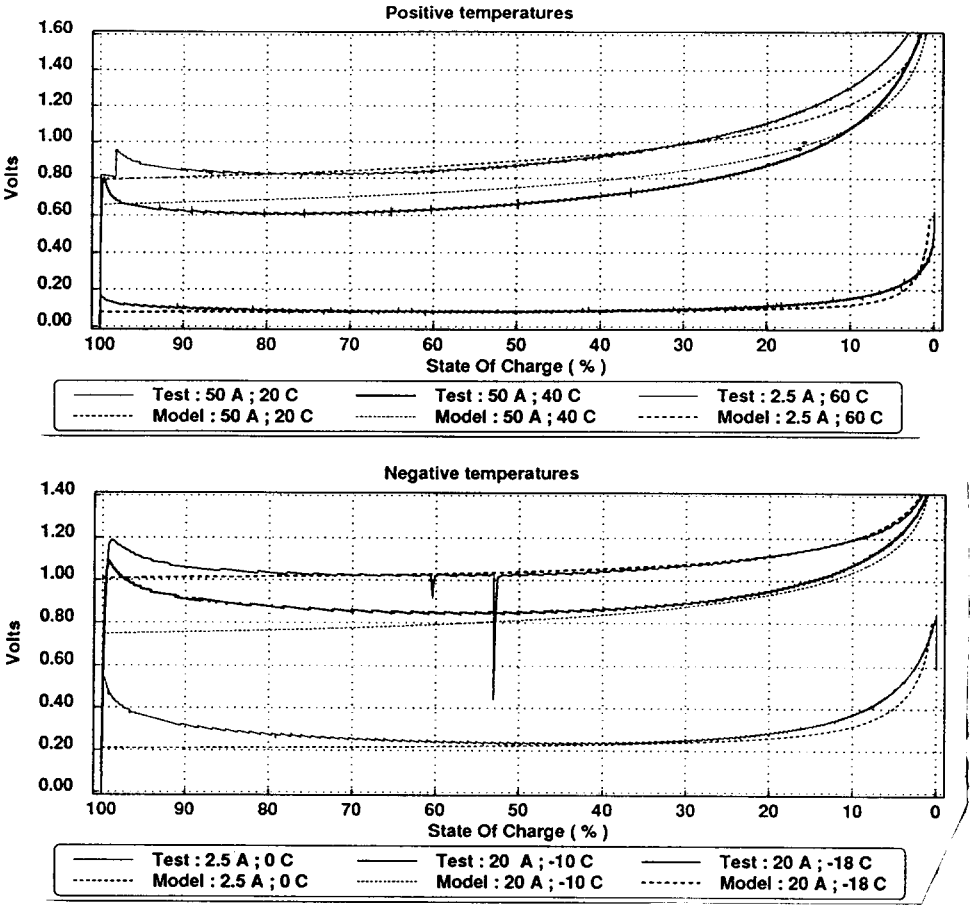

Fig. 6. Voltage drop law validation: comparison between test results and model.

To validate the e.m.f. law, self-discharge was taken into account at 60 °C in order to make an accurate evaluation. The e.m.f. discrepancies obtained are within 20 mV. For each discharge, a comparison between e.m.f. measurements (at the beginning and the end of the discharges) and the model confirmed that the test protocol and the equations are in good agreement (Table 1).

The difference between the validated e.m.f. law and the registered voltages was used to identify the parameters of the voltage-drop law. In some cases, internal temperature evolution during discharge had to be taken into account to calculate the e.m.f. (for cold discharge at 'high' current only) and the self-discharge at high temperature. To validate the electrical behaviour, each registered voltage curve was compared with the model

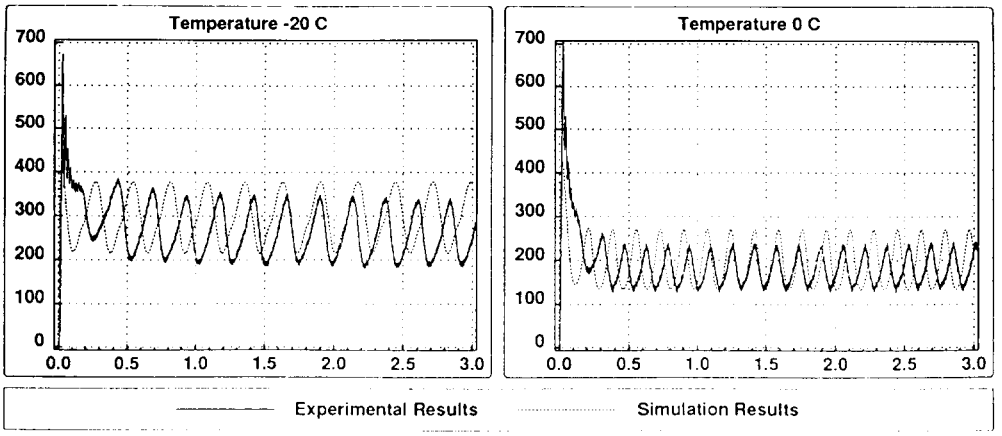

Fig. 7. F3N engine: starting phases validation. Battery current (A) vs. time (s).

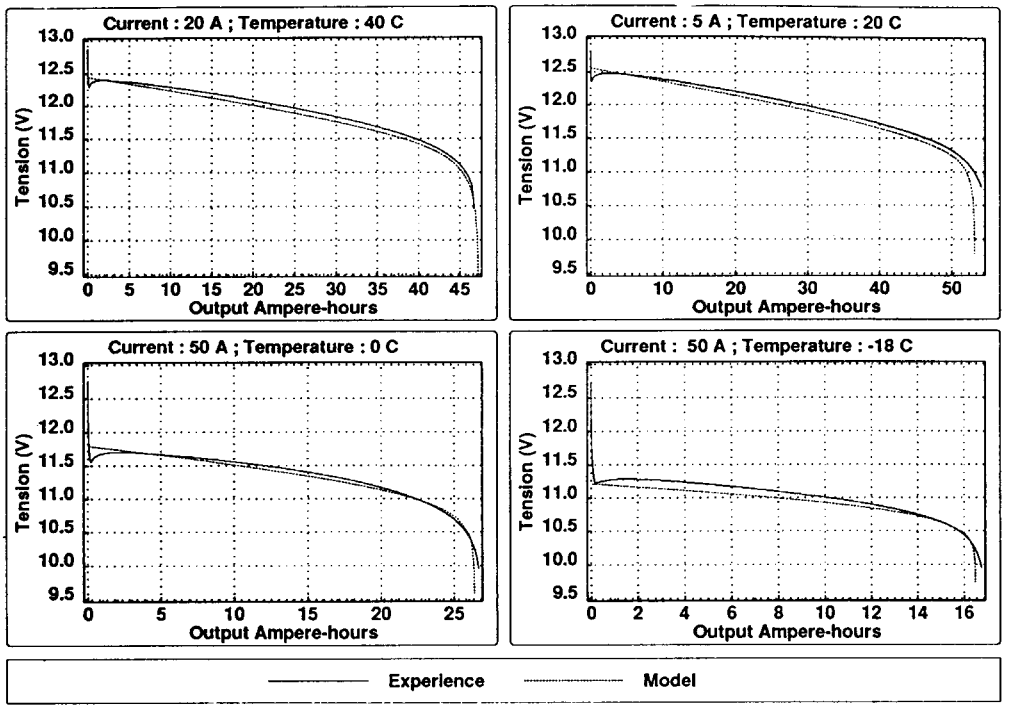

Fig. 8. Battery discharge model validation.

(Fig. 6). The voltage discrepancy was found to be within 7%. Good agreement is also given by the capacity law, namely, 5% (Table 2). Characteristics according to the technical specification [8] were reached, particularly during the starting phase.

The model provides the internal resistance and endurance values (at cold start) recommended by the manufacturer. It is now necessary to validate the charge model. The first simulations show that the behaviour of the battery charge model remains adequate.

4.2. Global validation

Three types of global validation are required:
(i) for starting phases;
(ii) with continuous and graduated discharge tests;
(iii) under vehicle running conditions.

Using the starter model and one engine model, simulated delivered currents were compared with experimental currents and voltage tests (Fig. 7). This model allows simulation of the starting phases with a good accuracy. It was confirmed that the model provides good results with respect to graduated and continuous discharges (Figs. 4 and 8, respectively).

Electric variables have also been registered on vehicles during city, road and highway running conditions. Comparison between simulations and experimental results shows that the network behaviour can be restored and good agreement with the battery model is obtained in discharge and charge modes (Fig. 9). As the battery state-of-charge is quite good on vehicles, the current that is crossing the battery is not too high. Thus, the

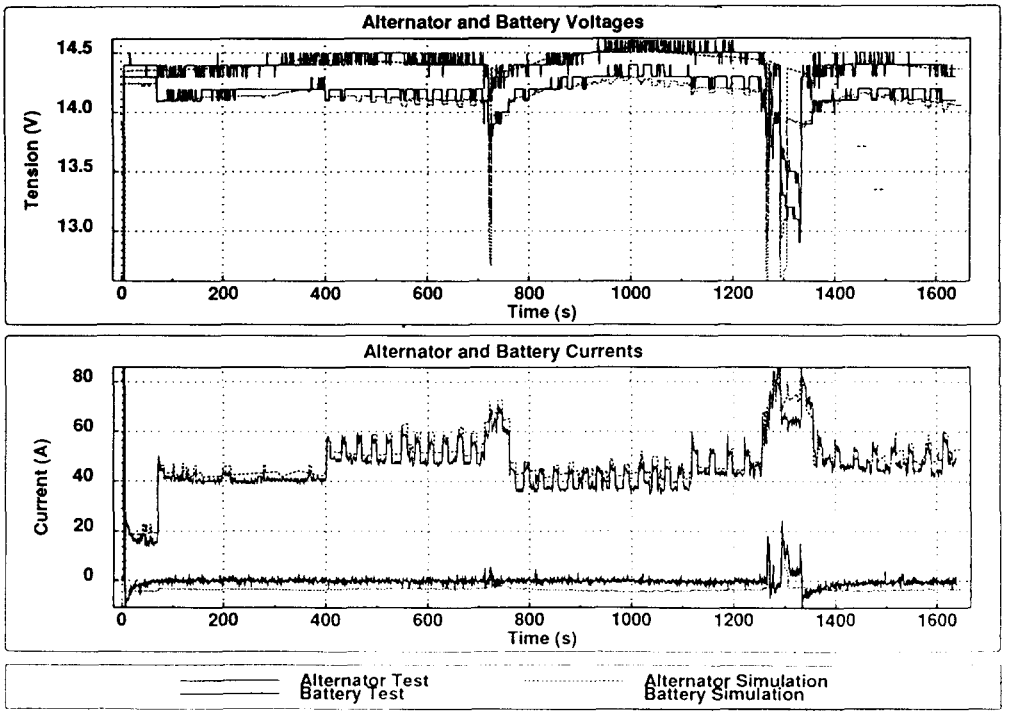

Fig. 9. Comparison between simulation and vehicle registrations; road cycle: 18.7 km.

battery charge model appears quite good, though it still has to be validated.

5. Conclusions

A behavioural model for automotive batteries has been developed to insert into simulation software. Compared with other models, it provides a good prediction of the vehicle electrical network in quasi-stationary states. The discharge model is independent of the battery technology that is used. The latter can be accommodated by different parameter values, coming from the identification discharge tests.

Model equations allow a good form of the charge curves to be developed. By charging the charge coefficient through detecting the sign of the current (i.e., charge or discharge), it is hoped to describe the charge behaviour with good accuracy. It is now necessary to find the right charge coefficients, to develop an experimental protocol in order to identify coefficients, and to validate the model under charge.

To extend the model for transient states, the different parts of the voltage discrepancy law should be separated and the capacity behaviour should be added. Thus, the model is open to future evolutions and will allow simulation of the transient states on the electrical network of a vehicle.

Acknowledgements

The author is grateful to A. Le Douaron and Ch. Brient (Renault, research department) for their help, to G. Chaumain (ADEME) for his cooperation in the project, to Professor M. Poloujadoff for his encouragement and directions, and to M. Jacques, C. Pascon (CEAC) and Pr Fauvarque (CNAM) for helpful discussions.

References

[1] H. Duval and C. Brient, Sirex, vehicle electric network simulation software, *SAE Congr., Detroit, MI, 1994,* No. 940132.
[2] H. Bode, *Lead Acid Batteries,* Wiley, New York, 1977.
[3] J. Meiwes, Etudes de la stratification de l'acide dans les batteries au plomb, *E.V.S. 7, Versailles, France, 1984,* pp. 41–46.
[4] A.J. Bard and L.R. Faulkner, *Electrochimie: Principes, Méthodes et Applications,* Masson, Paris, 1983.
[5] J. Bouet, Compréhension des mécanismes de charge de l'accumulateur au plomb, *Final Rep. NT.89.DEM/ELC.243/276.JB/SM,* Marcoussis Laboratory, Energetic Division, May 1989.
[6] R. Kaushik and I.G. Mawston, *J. Power Sources, 28* (1989) 161–169.
[7] J.L. McKinley and R.D. Brent, *Electricity and Electronics for Aerospace Vehicles,* McGraw Hill, New York, 1971.
[8] Lead acid batteries, requirement and test methods, *ISO/CEI 95-1,* 1988.